Demonstration of meta-signal positioning using LAMBDA ambiguity fixing method within a bit-true simulation

M. S. Hameed, T. Pany, *Universität der Bundeswehr München Germany*

T. Woerz, J. Wendel, *Airbus Defence and Space GmbH*

M. Paonni, T. Senni, *Joint Research Center, European Commission*

Presentation Outline

1. Motivation
    1. Meta-signals : tracking of wide-band signals for improved positioning
    2. High-order BOC tracking schemes
    3. Sub-carrier ambiguity fixing in position domain
2. Meta-signal positioning engine
    1. Observation model
    2. KF filter
    3. LAMBDA-method based sub-carrier ambiguity resolution
3. Simulation and test set-up
    1. Signal generation and tracking
    2. Test cases
4. Positioning results
    1. Filter parameters
    2. Testcase 1 : no multipath
    3. Testcase 2 : simulated dynamic multipath
    4. Testcase 3 : strong static multipath
    5. Analysis
5. Conclusions
6. References

1. Motivation

1.1 Meta-signals : tracking of wide-band signals for improved positioning

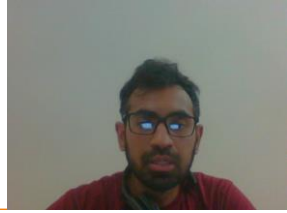

- *Meta-signal* : corresponds to the prospect of tracking two signals on different carrier frequencies as one wideband signal.

- Enables ‘sub-carrier’ tracking exhibiting a performance with low tracking jitter due to extremely narrow correlation peak.

- Sub-carrier tracking produces ‘sub-carrier’ phase observations – precise up to cm level but ambiguous up to integer multiple of sub-carrier wavelength.

- Sub-carrier tracking realizes positioning with improved accuracy especially under urban canyon multipath conditions without the requirement of a reference station.

- Meta-signals can be approximated as high-order BOC signals, invoking interest in optimal high-order BOC tracking schemes.

1.2 High-order BOC tracking schemes

Problem statement : *For BOC modulation, besides the tracking point on the main peak, the ACF consists of several other stable tracking points due to the presence of side-peaks. For meta-signals, approximated as high-order BOC signals, the amplitudes of consecutive side-peaks only slightly differ resulting in false locks.*

Bump Jump:

- Besides the three E-P-L correlators, it employs two additional correlators: the Very Early (VE) and Very Late (VL) correlators.
- A false lock is said to be occurring if there exists a significant difference between VE and VL correlator values over a given time duration.
- Scheme fails for high-order BOC signals.

Double-estimator

- Besides DLL and PLL, a Sub-carrier Lock Loop (SLL) is implemented which uses a sub-carrier replica for correlation after the PRN code is wiped-off by the DLL.
- Using SLL code phase, pseudoranges are obtained which are very precise but ambiguous i.e the tracking jitter in the SLL output is very small but the tracked sub-carrier position within a given PRN code sequence is not known.
- If DLL measurement noise is within a half sub-carrier wavelength, then code observations can be directly be used to resolve sub-carrier ambiguity.
- Ineffective alone in absence of ambiguity fixing filter especially when there is high code noise for e.g in urban canyon environment.

1.3 Sub-carrier ambiguity fixing in position domain

- Sub-carrier phase : a navigation observable similar to carrier phase → precise but ambiguous upto an integer multiple of sub-carrier wavelength.
- Sub-carrier wavelength → in order of a few meters → ambiguity can be resolved by conditioning sub-carrier observations on filtered code observations → no requirement of a reference receiver.
- Ambiguity resolved using a combined code and sub-carrier observation model.
- Obtained position solution accurate upto cm level.
- High-applicabilty in urban canyon multipath environments for commercial receiver market.
- To demonstrate this, this research is conducted by ISTA UniBwM in collaboration with Airbus Defence & Space as part of FUNTIMES II project within the H2020 Framework funded by the Eurpoean Commision.

2. Meta-signal positioning engine

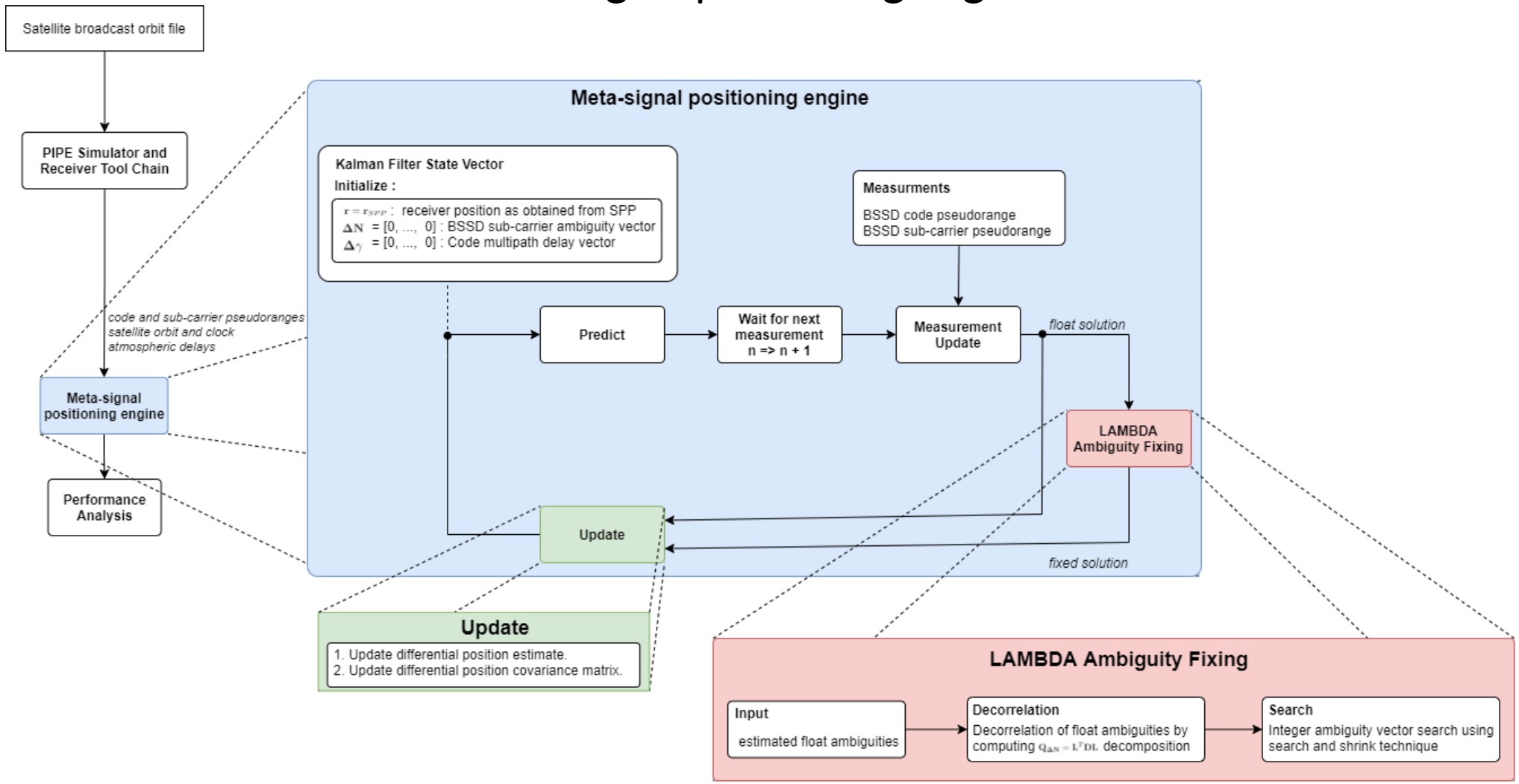

2.1 Observation model

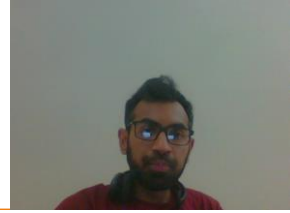

Code and sub-carrier observation equations

The following code $\tilde{\rho}^k$ and sub-carrier $\tilde{\phi}^k$ observation models are considered:

$$\tilde{\rho}^k = \left\| \mathbf{r}^{\vec{k}} - \vec{\mathbf{r}} \right\| + c\left(\delta\tau - (\delta\tau^k + \delta\tau^k_{rel})\right) + T^k + I^k + \gamma^k + \nu^k_\rho$$

non-standard extension

$$\tilde{\phi}^k = \left\| \mathbf{r}^{\vec{k}} - \vec{\mathbf{r}} \right\| + c\left(\delta\tau - (\delta\tau^k + \delta\tau^k_{rel})\right) + N^k\lambda + T^k + I^k + \nu^k_\phi$$

$\overrightarrow{\mathbf{r}^k}$: satellite position
$\vec{\mathbf{r}}$: receiver position
$\delta\tau$: receiver clock offset
$\delta\tau^k$: satellite clock offset
$\delta\tau^k_{rel}$: satellite clock relativity term
T^k : tropospheric delay in meters
I^k: ionospheric delay in meters
ν^k_ρ : code noise
ν^k_ϕ: sub-carrier noise
N^k : integer ambiguity
λ : sub-carrier wavelength

BSSD obervations

To eliminate receiver clock offset, BSSD observations are considered:

$$\bar{\rho}^k = (\tilde{\rho}^k - \rho^k) - (\tilde{\rho}^0 - \rho^0) = -\left(\left(\mathbf{e}^{\vec{k}}\right)^T + \left(\mathbf{e}^{\vec{0}}\right)^T\right)\vec{\mathbf{r}} + \Delta\gamma^k + \nu^k_\rho - \nu^0_\rho$$

$$\bar{\phi}^k = \left(\tilde{\phi}^k - \phi^k\right) - \left(\tilde{\phi}^0 - \phi^0\right) = -\left(\left(\mathbf{e}^{\vec{k}}\right)^T + \left(\mathbf{e}^{\vec{0}}\right)^T\right)\vec{\mathbf{r}} + \Delta N^k\lambda + \nu^k_\phi - \nu^0_\phi$$

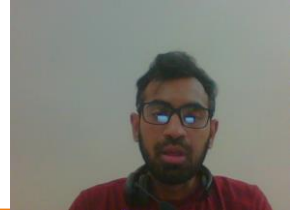

2.1 Observation model contd.

Combined BSSD code and sub-carrier observation model for K satellites

$\mathbf{y} = \mathbf{H}\vec{\mathbf{r}} + \mathbf{A}\begin{pmatrix}\mathbf{\Delta N}\\ \mathbf{\Delta}\gamma\end{pmatrix} + \epsilon_{\mathbf{y}}$: combined observation model

$\mathbf{y} = \begin{pmatrix}\bar{\rho^1}\\ .\\ .\\ \bar{\rho^k}\\ \bar{\phi^1}\\ .\\ .\\ \bar{\phi^k}\end{pmatrix}$: measurement vector

$\mathbf{\Delta N} = \begin{pmatrix}\Delta N^1\\ .\\ .\\ \Delta N^{K-1}\end{pmatrix}$: BSSD sub-carrier ambiguity vector

$\mathbf{\Delta}\gamma = \begin{pmatrix}\Delta\gamma^1\\ .\\ .\\ \Delta\gamma^{K-1}\end{pmatrix}$: BSSD code multipath vector

$\mathbf{H} = \begin{pmatrix}-\left(\left(\vec{\mathbf{e}^1}\right)^T + \left(\vec{\mathbf{e}^0}\right)^T\right)\\ .\\ .\\ -\left(\left(\vec{\mathbf{e}^{K-1}}\right)^T + \left(\vec{\mathbf{e}^0}\right)^T\right)\\ -\left(\left(\vec{\mathbf{e}^1}\right)^T + \left(\vec{\mathbf{e}^0}\right)^T\right)\\ .\\ .\\ -\left(\left(\vec{\mathbf{e}^{K-1}}\right)^T + \left(\vec{\mathbf{e}^0}\right)^T\right)\end{pmatrix}$: geometry matrix

$\mathbf{A}_\lambda = \begin{pmatrix}\mathbf{0}_{(K-1)(K-1)}\\ \lambda\mathbf{I}_{(K-1)(K-1)}\end{pmatrix}$: ambiguity state coefficient matrix

$\mathbf{A}_\gamma = \begin{pmatrix}\mathbf{I}_{(K-1)(K-1)}\\ \mathbf{0}_{(K-1)(K-1)}\end{pmatrix}$: code multipath state coefficient matrix

$\mathbf{A} = (\mathbf{A}_\lambda, \mathbf{A}_\gamma)$

2.2 Kalman filter

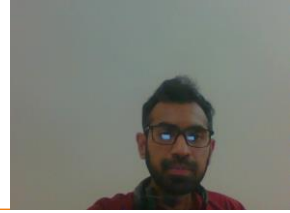

Kalman Filter

For positioning, a closed-loop Kalman filter is used to estimate offsets that need to be added to the estimated receiver position, BSSD sub-carrier ambiguities and BSSD code multipath delays, so that they converge to the true values over time.

$$\mathbf{x} = \begin{pmatrix} \delta x \\ \delta y \\ \delta z \\ \delta\Delta N^1 \\ \cdot \\ \cdot \\ \delta\Delta N^{K-1} \\ \delta\Delta\gamma^1 \\ \cdot \\ \cdot \\ \delta\Delta\gamma^{K-1} \end{pmatrix}$$: state vector

$$\mathbf{Q} = \begin{pmatrix} \Phi_r & & & & & & & & \\ & \Phi_r & & & & & & & \\ & & \Phi_r & & & \mathbf{0} & & & \\ & & & \Phi_{\Delta N} & & & & & \\ & & & & \cdot & & & & \\ & & & & & \Phi_{\Delta N} & & & \\ & & \mathbf{0} & & & & \Phi_\gamma & & \\ & & & & & & & \cdot & \\ & & & & & & & & \Phi_\gamma \end{pmatrix}$$: state process noise matrix

where Φ_r : position state process noise
$\Phi_{\Delta N}$: sub-carrier ambiguity process noise
Φ_γ : code multipath process noise

$$\mathbf{R} = \begin{pmatrix} \mathbf{D}\mathbf{R}_\rho\mathbf{D}^T & \\ & \mathbf{D}\mathbf{R}_\phi\mathbf{D}^T \end{pmatrix}$$: measurement noise matrix

$$\mathbf{D} = \begin{pmatrix} 1 & -1 & & \\ 1 & & \cdot & \\ \cdot & & & \cdot \\ \cdot & & & \\ 1 & & & -1 \end{pmatrix}$$: single-difference matrix

$\mathbf{R}_\rho = diag(2\sigma_\rho^{1^2}, ..., 2\sigma_\rho^{K-1^2})$: code measurement noise matrix

$\mathbf{R}_\phi = diag(2\sigma_\phi^{1^2}, ..., 2\sigma_\phi^{K-1^2})$: sub-carrier measurement noise matrix

$\mathbf{F} = (\mathbf{H}, \mathbf{A})$: system matrix

$$\mathbf{P}_0 = \begin{pmatrix} \sigma_{dx}^2 & & & & & & & & \\ & \sigma_{dy}^2 & & & & & & & \\ & & \sigma_{dz}^2 & & & \mathbf{0} & & & \\ & & & \sigma_{N^1}^2 & & & & & \\ & & & & \cdot & & & & \\ & & & & & \sigma_{N^{K-1}}^2 & & & \\ & & \mathbf{0} & & & & \sigma_{\gamma^1}^2 & & \\ & & & & & & & \cdot & \\ & & & & & & & & \sigma_{\gamma^{K-1}}^2 \end{pmatrix}$$: state covariance matrix

where $[\sigma_{dx}^2 \sigma_{dy}^2 \sigma_{dz}^2]$: position state variances
$\sigma_{N^k}^2$: sub-carrier ambiguity process noise
$\sigma_{\gamma^k}^2$: code multipath process noise

Kalman filter update steps

1. Filter Time update (predict)

$$\mathbf{x}_i^- = \mathbf{\Phi}\mathbf{x}_{i-1}$$

$$\mathbf{P}_i^- = \mathbf{\Phi}\mathbf{P}_{i-1}\mathbf{\Phi}^\mathbf{T} + \mathbf{Q}$$

2. Filter Measurement update

$$\mathbf{z}_i = \mathbf{y}_i - \mathbf{F}\mathbf{x}_i^-$$

$$\mathbf{K}_i = \mathbf{P}_i^-\mathbf{F}\left(\mathbf{F}\mathbf{P}_i^-\mathbf{F}^T + \mathbf{R}\right)^{-1}$$

$$\mathbf{x}_i^+ = \mathbf{x}_i^- + \mathbf{K}_i\mathbf{z}_i$$

$$\mathbf{P}_i^+ = \left(\mathbf{I} - \mathbf{K}_i\mathbf{F}\right)\mathbf{P}_i^-$$

2.3 LAMBDA-method based sub-carrier ambiguity resolution

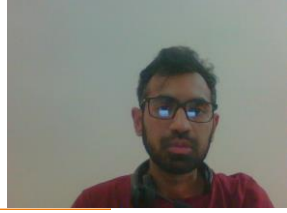

LAMBDA ambiguity fixing

The integer ambiguity within the sub-carrier pseudorange observations are resolved using LAMBDA ambiguity fixing method:

1. Decorrelation of float ambiguities

a) Cholesky decomposition

Decomposition of the float ambiguity covariance matrix $\mathbf{Q_{\Delta N}}$ into a lower triangular matrix $\mathbf{L}$ and a diagonal matrix $\mathbf{D}$ as:

$$\mathbf{Q_{\Delta N}} = \mathbf{L}^T \mathbf{D} \mathbf{L}$$

b) Reparameterization using Z-transform

A reparameterization of the ambiguities is then done by computing the Z-transform matrix $\mathbf{Z}$ through an iterative process

$$\bar{\mathbf{z}} = \mathbf{Z}^T \bar{\mathbf{\Delta N}}$$

$$\mathbf{Q_z} = \mathbf{Z}^T \mathbf{Q_{\Delta N}} \mathbf{Z}$$

2. Search of integer ambiguity vector

The integer estimate is obtained through a search over the integer grid points of an n-dimensional hyper-ellipsoid which has a size defined by a positive constant X^2, is centred at $\hat{\mathbf{z}}$ and is shaped by the covariance matrix $\mathbf{Q_z}$

$$\tilde{\mathbf{z}} = \arg\ min\, (\bar{\mathbf{z}} - \mathbf{z})^T\, \mathbf{Q_z}^{-1}\, (\bar{\mathbf{z}} - \mathbf{z})$$

$$F\,(\tilde{\mathbf{z}}) = (\bar{\mathbf{z}} - \mathbf{z})^{\mathbf{T}}\, \mathbf{Q_z}^{-1}\, (\bar{\mathbf{z}} - \mathbf{z}) \leq X^2$$

3. Back-transformation of fixed ambiguities

After the search process is completed, the fixed ambiguity vector is finally obtained by taking the inverse Z-transform of the searched solution

$$\widetilde{\mathbf{\Delta N}} = \mathbf{Z}^{-T} \tilde{\mathbf{z}}$$

2.3 LAMBDA-method based sub-carrier ambiguity resolution contd.

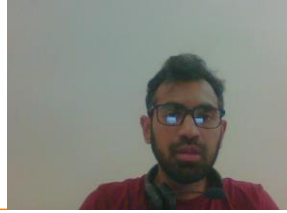

3. Fixed solution validation

The ratio and difference are compared against their thresholds respectively. Whenever, the thresholds are crossed, a simple rounded solution of the float ambiguity vector (before decorrelation) is taken as the fixed.

$$ratio = \frac{(\widetilde{\mathbf{\Delta N}}_2 - \mathbf{\Delta N})^T \mathbf{Q_{\Delta N}}^{-1} (\widetilde{\mathbf{\Delta N}}_2 - \mathbf{\Delta N})}{(\widetilde{\mathbf{\Delta N}}_1 - \mathbf{\Delta N})^T \mathbf{Q_{\Delta N}}^{-1} (\widetilde{\mathbf{\Delta N}}_1 - \mathbf{\Delta N})} > \mu_{ratio}$$

$$difference = (\widetilde{\mathbf{\Delta N}}_2 - \mathbf{\Delta N})^T \mathbf{Q_{\Delta N}}^{-1} (\widetilde{\mathbf{\Delta N}}_2 - \mathbf{\Delta N}) - (\widetilde{\mathbf{\Delta N}}_1 - \mathbf{\Delta N})^T \mathbf{Q_{\Delta N}}^{-1} (\widetilde{\mathbf{\Delta N}}_1 - \mathbf{\Delta N}) > \mu_{diff}$$

$$\widetilde{\mathbf{\Delta N}} = round(\mathbf{\Delta N})$$

If ambiguity validation is successful, the fixed solution is used to update the differential position states and its covariance matrix

$$\begin{pmatrix} \delta x \\ \delta y \\ \delta z \end{pmatrix}^+ = \left(\mathbf{H^T Q_y}^{-1} \mathbf{H}\right) \mathbf{H^T Q_y}^{-1} \left(\mathbf{y} - \mathbf{A}_\lambda \left(\widetilde{\mathbf{\Delta N}} - \mathbf{\Delta N}\right)\right)$$

$$\mathbf{P}_{[1,2,3;1,2,3]} = \mathbf{P}_{[1,2,3;1,2,3]} - \mathbf{Q_{r\Delta N} Q_{\Delta N}^{-1} Q^T}_{\mathbf{r\Delta N}}$$

Absolute receiver position, BSSD sub-carrier ambiguities and BSSD code multipath estimates are updated using either float or fixed solution.

$$\mathbf{r}_i = \mathbf{r}_{i-1} + \begin{pmatrix} \delta x \\ \delta y \\ \delta z \end{pmatrix}_i^+$$

$$\mathbf{\Delta N}_i = \mathbf{\Delta N}_{i-1} + \begin{pmatrix} \delta \Delta N^1 \\ \cdot \\ \cdot \\ \delta \Delta N^{K-1} \end{pmatrix}_i^+$$

$$\mathbf{\Delta \gamma}_i = \mathbf{\Delta \gamma}_{i-1} + \begin{pmatrix} \delta \Delta \gamma^1 \\ \cdot \\ \cdot \\ \delta \Delta \gamma^{K-1} \end{pmatrix}_i^+$$

3. Simulation set-up

3.1 Signal generation and tracking

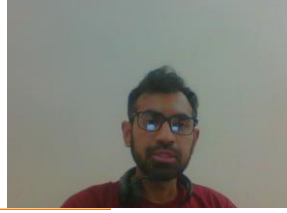

- PIPE consists of a full constellation bit-true GNSS signal simulator at IF sample level.
- The PIPE simulator takes input a navigation data record file and for a user-defined receiver position it produces the output of meta-signal tracking in .csv format.
- PIPE_csv file contains timestamps, code and sub-carrier pseudoranges , satellite orbit and clock parameters and modelled atmospheric delay terms (broadcast group delay, ionosphere and troposphere).
- PIPE_csv2rinex script was developed to perform the necessary file conversion.

RINEX File

```
     3.03           OBSERVATION DATA    Mixed(MIXED)         RINEX VERSION / TYPE
LAMBDA SIM TOOL                                              PGM / RUN BY / DATE
------------------------------------------------------------ COMMENT
BUILDING41                                                   MARKER NAME
ILDING41                                                     MARKER NUMBER
GEODETIC                                                     MARKER TYPE
GNSS Observer       Trimble                                  OBSERVER / AGENCY
5628R50286          AIRBUS-PIPE SIM       5.22               REC # / TYPE / VERS
                    TRM57971.00     NONE                     ANT # / TYPE
  4181672.3073   861029.3919  4723395.1598                   APPROX POSITION XYZ
        0.0000        0.0000        0.0000                   ANTENNA: DELTA H/E/N
E    2 C1X U1X                                               SYS / # / OBS TYPES
     1.000                                                   INTERVAL
     0                                                       RCV CLOCK OFFS APPL
G L2X -0.25000                                               SYS / PHASE SHIFT
R L1P  0.25000                                               SYS / PHASE SHIFT
R L2C -0.25000                                               SYS / PHASE SHIFT
    18                                                       LEAP SECONDS
DBHZ                                                         SIGNAL STRENGTH UNIT
                                                             END OF HEADER
> 2019  7  2 14 11 37.0000000  0  9
E01 26839131.920   26839130.510
E03 25406576.620   25406580.560
E05 27640367.210   27640364.050
E08 24356242.170   24356238.140
E13 23560848.080   23560845.190
E15 23956214.150   23956212.700
E21 25765985.470   25765982.200
E26 25924041.830   25924039.500
E27 27351772.090   27351773.040
> 2019  7  2 14 11 38.0000000  0  9
E01 26838952.390   26838952.950
E03 25406438.970   25406444.530
E05 27640699.340   27640701.550
E08 24355694.170   24355696.210
E13 23560672.960   23560669.120
E15 23956481.540   23956476.590
E21 25766318.700   25766314.100
E26 25923581.060   25923586.780
E27 27352383.840   27352377.490
> 2019  7  2 14 11 39.0000000  0  9
E01 26838770.260   26838775.230
E03 25406314.340   25406308.590
E05 27641035.290   27641038.880
E08 24355154.060   24355154.650
E13 23560495.430   23560493.060
E15 23956744.990   23956740.490
E21 25766647.090   25766645.880
E26 25923142.180   25923133.930
E27 27352981.000   27352982.030
```

Code pseudorange measurements

Sub-carrier pseudorange measurements

```
0.04000000, 9, 0.00400000, 0.00400000, 0.00000000, 0, 0.04205960, (
0.06000000, 14, 0.00400000, 0.00400000, 0.00000000, 0, 0.06205937,
0.08000000, 19, 0.00400000, 0.00400000, 0.00000000, 0, 0.08205917,
0.10000000, 24, 0.00400000, 0.00400000, 0.00000000, 0, 0.10205897,
0.12000000, 29, 0.00400000, 0.00400000, 0.00000000, 0, 0.12205877,
0.14000000, 34, 0.00400000, 0.00400000, 0.00000000, 0, 0.14205857,
0.16000000, 39, 0.00400000, 0.00400000, 0.00000000, 0, 0.16205837,
0.18000000, 44, 0.00400000, 0.00400000, 0.00000000, 0, 0.18205817,
0.20000000, 49, 0.00400000, 0.00400000, 0.00000000, 0, 0.20205797,
0.22000000, 54, 0.00400000, 0.00400000, 0.00000000, 0, 0.22205773,
0.24000000, 59, 0.00400000, 0.00400000, 0.00000000, 0, 0.24205753,
0.26000000, 64, 0.00400000, 0.00400000, 0.00000000, 0, 0.26205733,
0.28000000, 69, 0.00400000, 0.00400000, 0.00000000, 0, 0.28205713,
0.30000000, 74, 0.00400000, 0.00400000, 0.00000000, 0, 0.30205693,
0.32000000, 79, 0.00400000, 0.00400000, 0.00000000, 0, 0.32205673,
0.34000000, 84, 0.00400000, 0.00400000, 0.00000000, 0, 0.34205653,
0.36000000, 89, 0.00400000, 0.00400000, 0.00000000, 0, 0.36205630,
0.38000000, 94, 0.00400000, 0.00400000, 0.00000000, 0, 0.38205610,
```

PIPE CSV File

PIPE_csv2rinex

3.2 Test cases

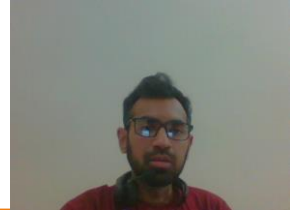

- Meta-signal generated as a BOC(1,1) + BOC(10.75,1) signal using Airbus PIPE simulator.

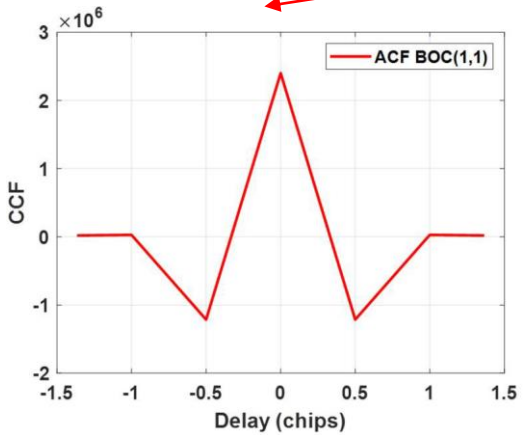

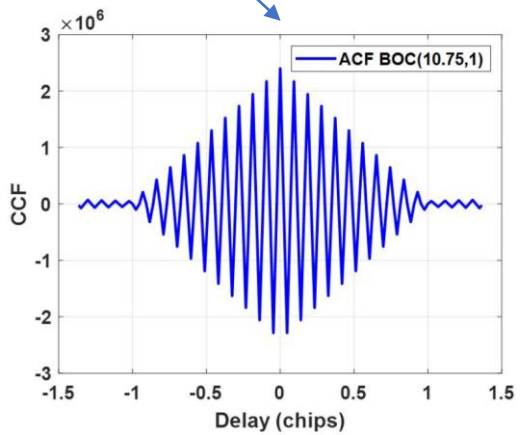

Testcase index	Multipath set-up
1	Multipath free test case with 08 satellites characterized by no multipath on code and sub-carrier observations
2	Dynamic multipath on all of the 08 satellites simulated as White Gaussian noise characterized by $\mathcal{N}(0, \sigma_C)$ for code and $\mathcal{N}(0, \sigma_{SC})$ for sub-carrier observations where $\sigma_C = 10$ m and $\sigma_{SC} = 0.03$ m
3	Strong static multipath on 05 out of 08 satellites with code bias upto 40 m

Testcase 3 – Strong static multipath

PRN Number	Relative Amplitude	Relative Delay [m]	Relative Phase [rad]
01	0.9	90.0	0.0
03	0.9	100.0	0.0
08	0.9	120.0	π
15	0.9	70.0	π
21	0.9	60.0	0.0

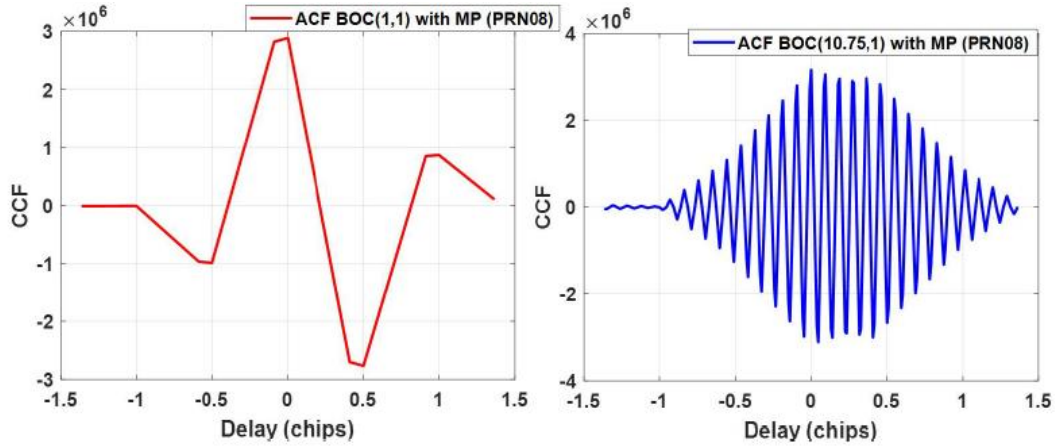

4. Positioning results

4.1 Filter parameters

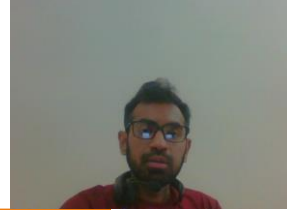

Parameter	Symbol	Value		
		Testcase 1	Testcase 2	Testcase 3
Initial position state variance	$\sigma^2_{dx}, \sigma^2_{dy}, \sigma^2_{dz}$	20^2 [m^2]	20^2 [m^2]	20^2 [m^2]
Initial ambiguity state variance	$\sigma^2_{N^k}$	$(10\lambda)^2$ [m^2]	$(10\lambda)^2$ [m^2]	$(10\lambda)^2$ [m^2]
Initial code multipath state variance	$\sigma^2_{\gamma^k}$	5^2 [m^2]	5^2 [m^2]	10^2 [m^2]
Position process noise	$\Phi_{\delta x}, \Phi_{\delta y}, \Phi_{\delta z}$	0.00015^2 [m^2]	0.00015^2 [m^2]	0.00015^2 [m^2]
Code multipath process noise	Φ_γ	1^2 [m^2]	1^2 [m^2]	5^2 [m^2]
Code measurement noise variance	σ^2_ρ	5^2 [m^2]	5^2 [m^2]	5^2 [m^2]
Sub-carrier measurement variance	σ^2_ϕ	0.088^2 [m^2]	0.088^2 [m^2]	0.088^2 [m^2]
Ambiguity resolution ratio threshold	μ_{ratio}	1	1	1
Ambiguity resolution difference threshold	μ_{diff}	0	$2.5e3$	$1e3$

- Parameters optimized for a static user in severe multipath conditions
- Only Galileo constellation taking into account
- For each test case, in a separate experimental run, the filter is reset after 10 secs every time a position fix is achieved to analyse filter stability.
- KPIs: time to successful subcarrier fixing, position accuracy after subcarrier fixing

4.2 Testcase 1 : no multipath

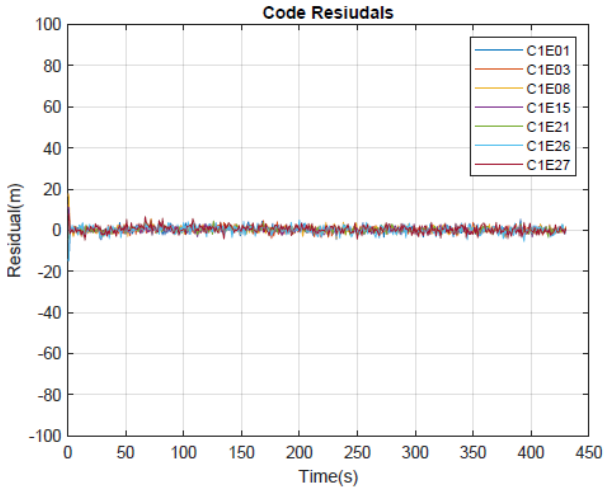

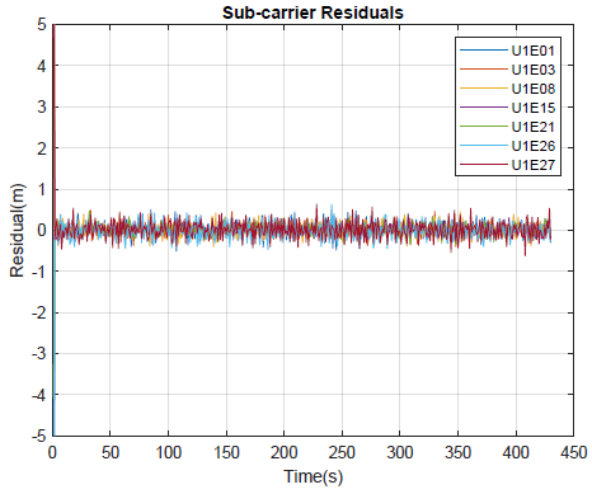

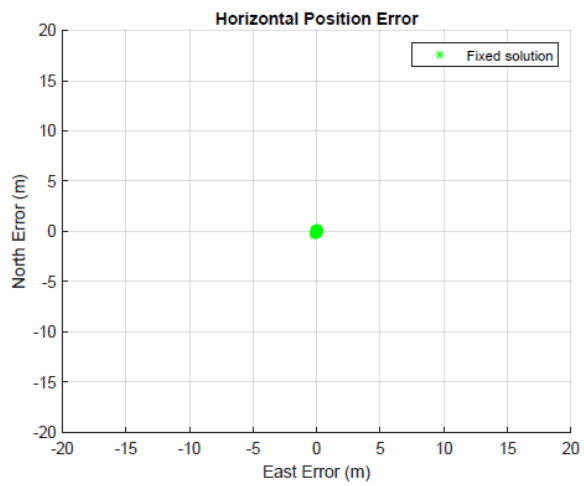

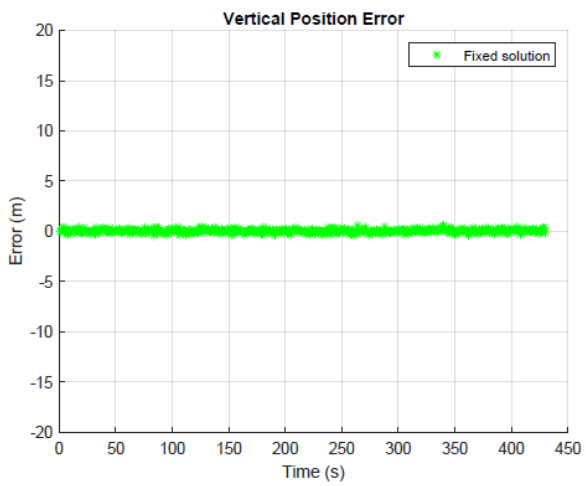

Without filter reset

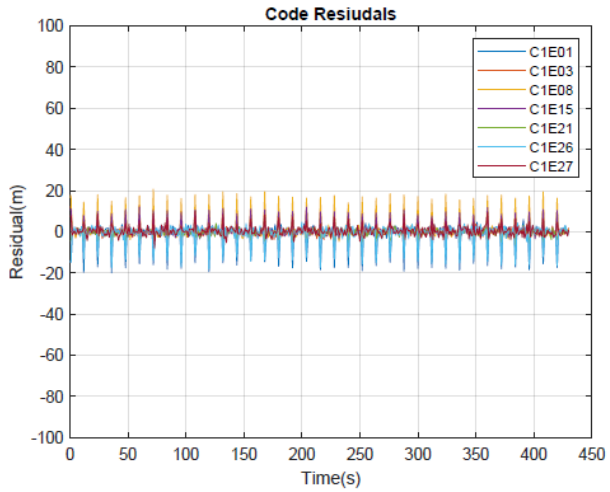

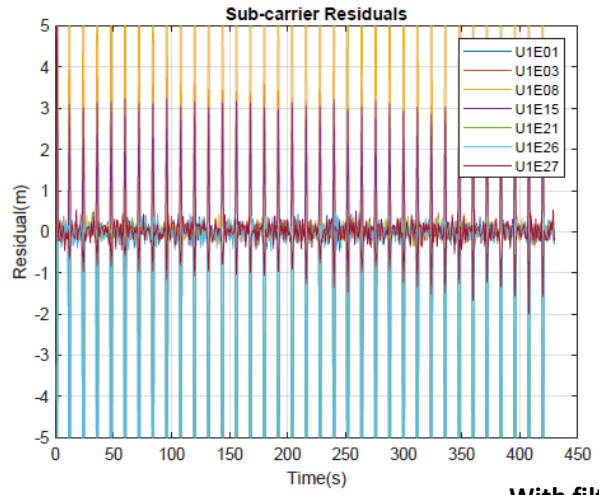

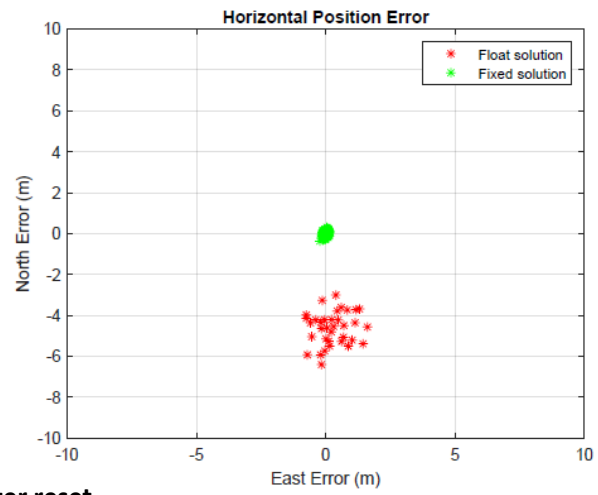

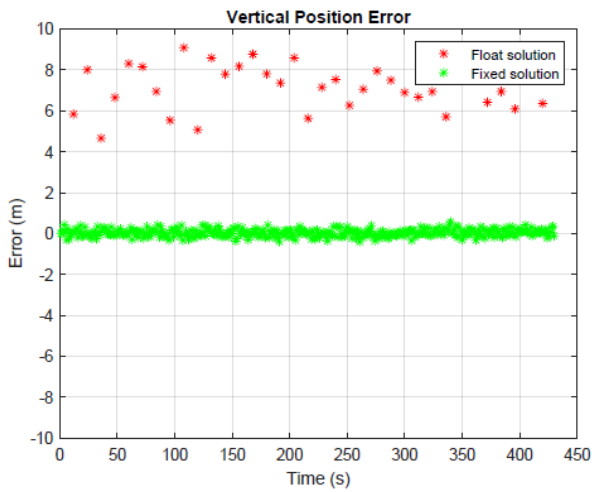

With filter reset

4.3 Testcase 2 : simulated dynamic multipath

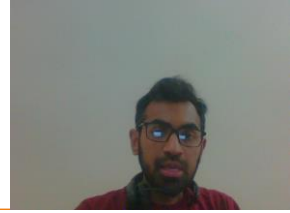

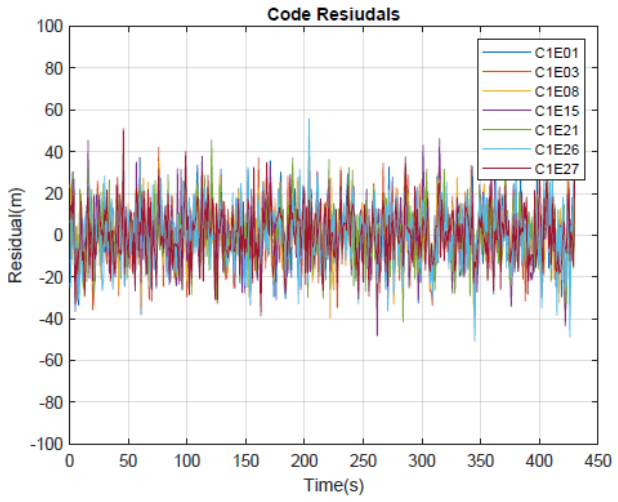

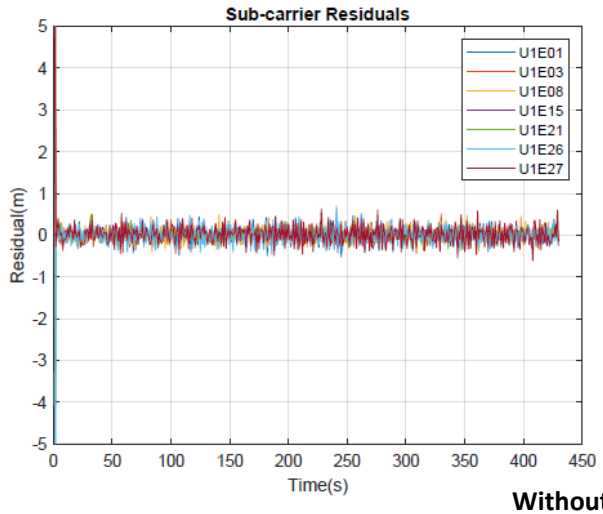

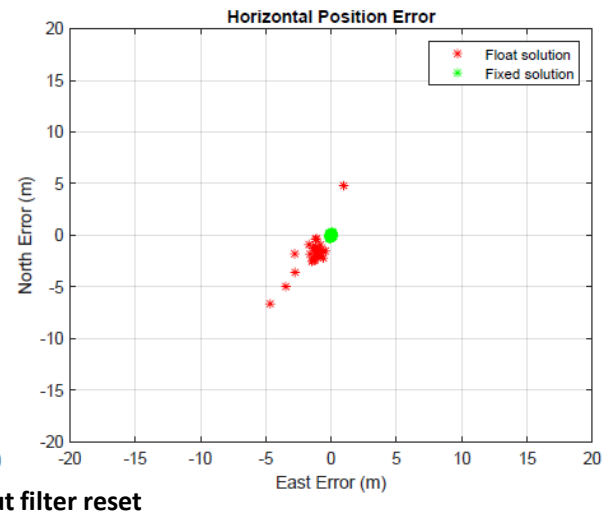

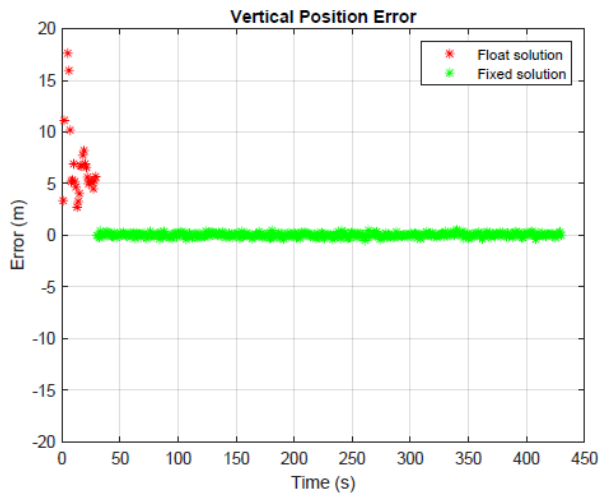

Without filter reset

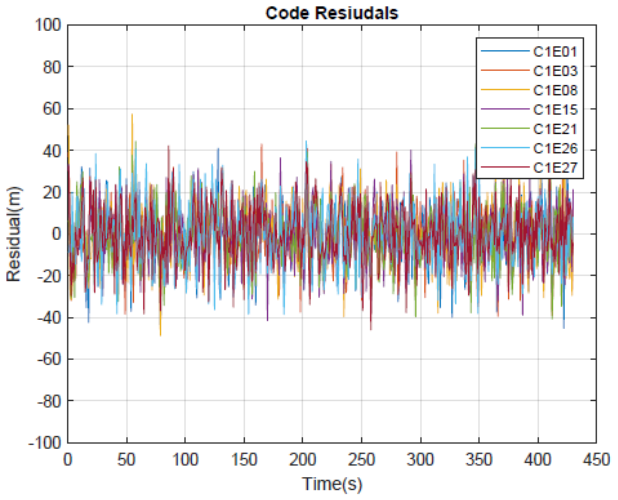

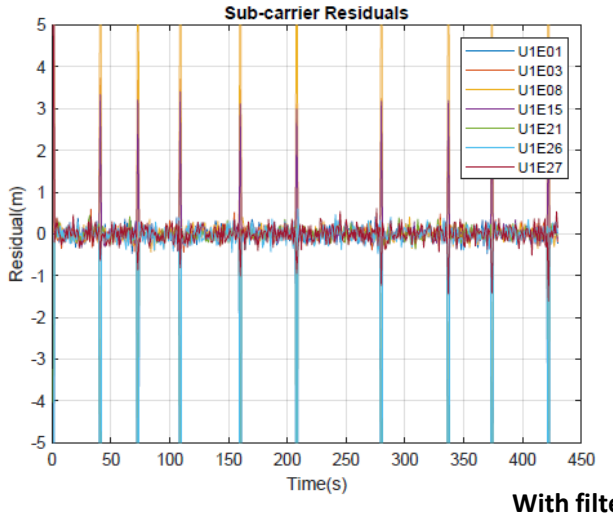

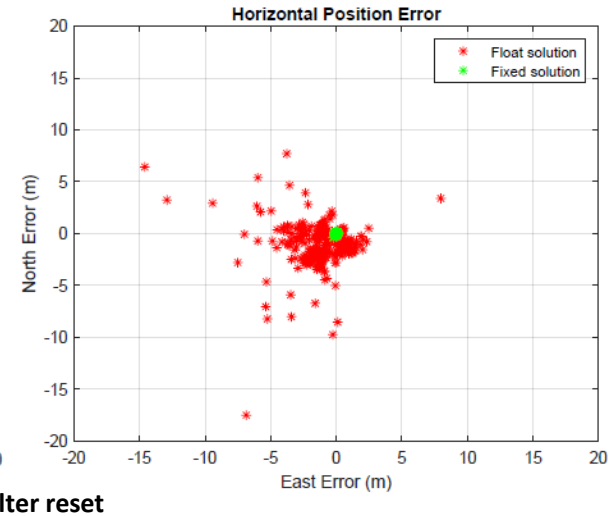

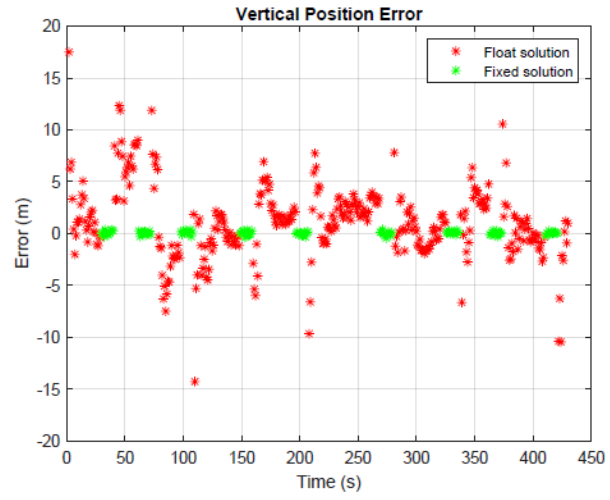

With filter reset

4.4 Testcase 3 : strong static multipath

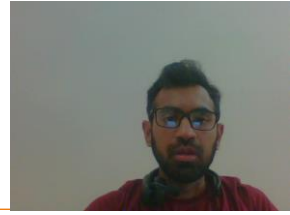

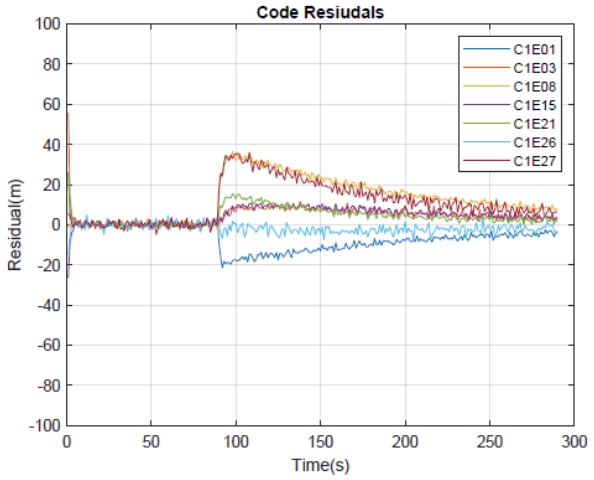

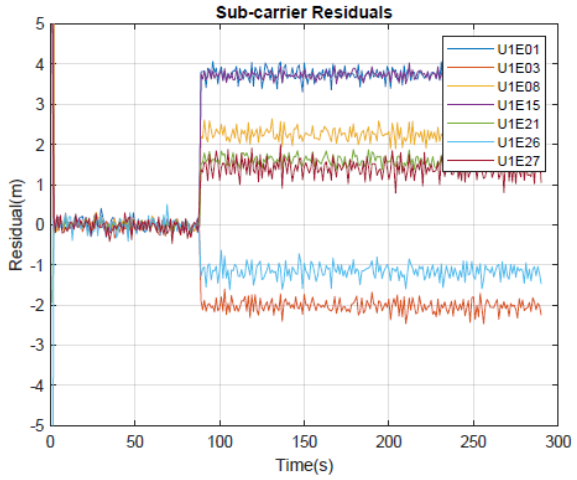

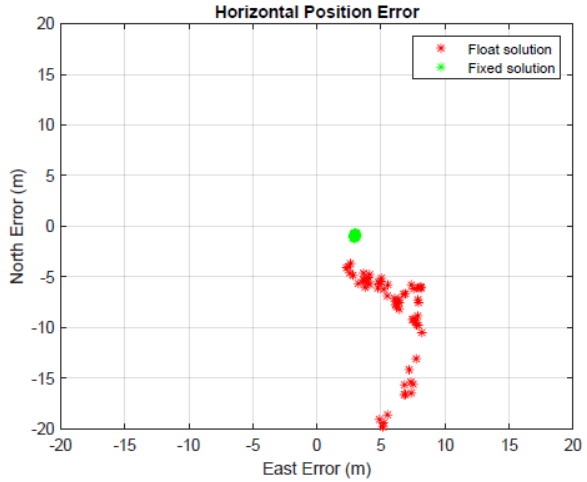

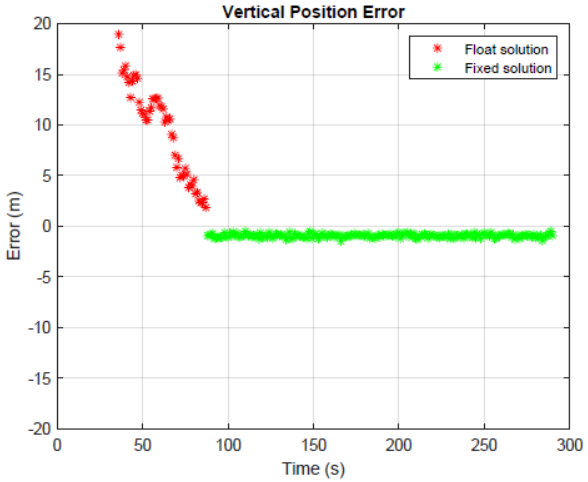

Without filter reset

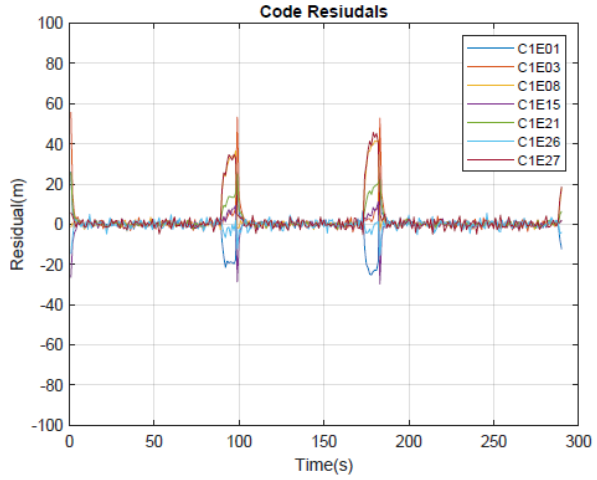

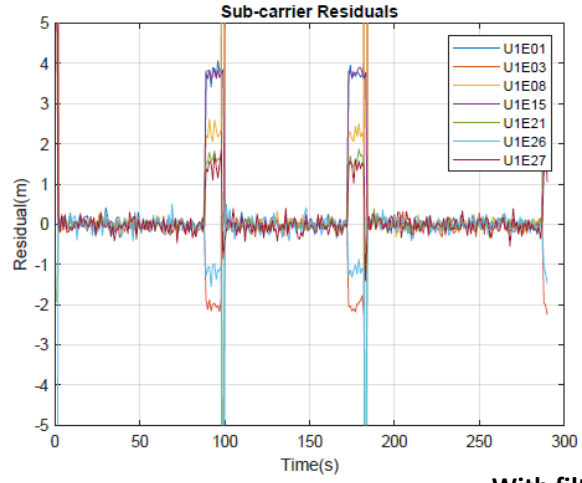

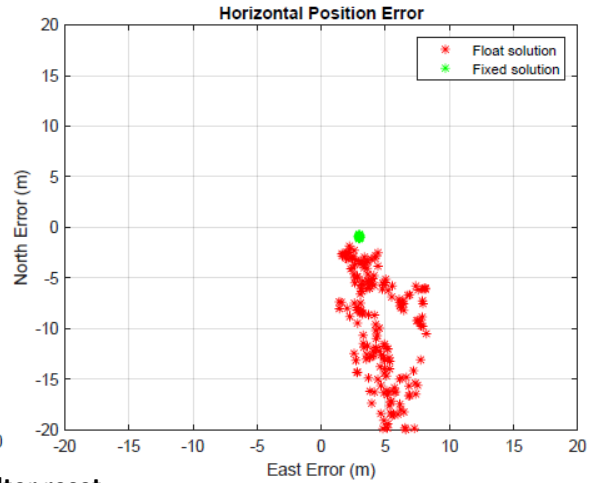

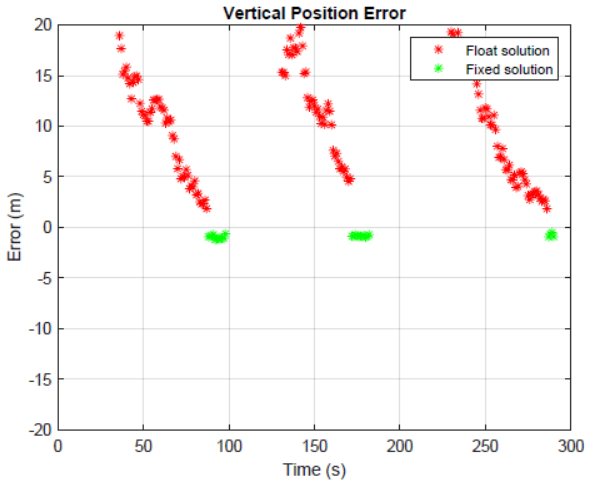

With filter reset

4.5 Analysis

Testcase 1 (no multipath)

- With no reset, all ambiguites instantaneously fixed to 0. With reset, all ambiguities are correctly fixed in the 2nd epoch after reset. It takes at least one epoch to compute the float ambiguities that need to be added as offsets to the absolute float ambiguity before fixing can take place.

Testcase 2 (dynamic – noise like – multipath)

- With no reset, all ambiguites instantaneously fixed to 0 at about t = 30 s. The code residuals are dominated by the code-multipath delay which in this case is White Gaussian noise.

Testcase 3 (strong static multipath

- As the ambiguities are fixed, all the error in the float solution is accumulated and distributed over the code MP states which produces a jump in the code residuals which then converges to the true static code MP values over time. After fixing, the position error is as accurate as the sub-carrier measurement noise.

- The sub-carrier residuals are biased after fixing due to the multipath delay present in the sub-carrier observations.

- With filter reset, the ambiguities are successfully fixed three times over the duration of the dataset. Since the code MP offset is in the order of 40m in this dataset, the filter convergence time is higher than the other two test cases.

5. Conclusions

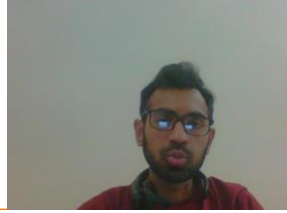

- LAMBDA ambiguity fixing can successfully resolve sub-carrier ambiguities even in high static-multipath scenarios given that a suitable filter is employed.
- Filter convergence time for correct ambiguity fixing is highly dependent on the quality of code observations → higher code multipath results in higher convergence time.
- Sub-carrier ambiguity resolution in position domain can realize dm level accurate position solutions without RTK i.e without a reference receiver.
- For standardizing the use of sub-carrier pseudoranges, the RINEX file format has to be updated with a dedicated sub-carrier observation tag.
- Sub-carrier fixing at range level with e.g. bump-jump or rounding of double-estimator SLL/DLL did show equal results for low multipath; there seems to be an improved performance of LAMBDA in high multipath but this does require further consolidation with multiple datasets (dynamic user, more realistic channel models etc)

6. References

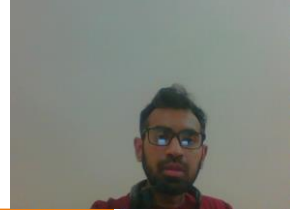

[1] M. Paonni, J. Curran, M. Bavaro, and J. Fortuny-Guasch, “Gnss meta signals: Coherently composite processing of multiple gnss signals,” in Proceedings of the 27th International Technical Meeting of the Satellite Division of The Institute of Navigation (ION GNSS+ 2014), 2014, pp. 2592–2601.

[2] J.-L. Issler, M. Paonni, and B. Eissfeller, “Toward centimetric positioning thanks to l-and s-band gnss and to meta-gnss signals,” in 2010 5th ESA Workshop on Satellite Navigation Technologies and European Workshop on GNSS Signals and Signal Processing (NAVITEC). IEEE, 2010, pp. 1–8.

[3] J. Wendel, F. M. Schubert, and S. Hager, “A robust technique for unambiguous boc tracking,” NAVIGATION, vol. 61, no. 3, pp. 179–190, 2014. [Online]. Available: https://onlinelibrary.wiley.com/doi/abs/10.1002/navi.62

[4] P. J. Teunissen, “Least-squares estimation of the integer gps ambiguities,” in Invited lecture, section IV theory and methodology, IAG general meeting, Be¼ing, China, 1993.

[5] P. De Jonge, C. Tiberius et al., “The lambda method for integer ambiguity estimation: implementation aspects,” Publications of the Delft Computing Centre, LGR-Series, vol. 12, no. 12, pp. 1–47, 1996.

[6] L.Wang and S. Verhagen, “A new ambiguity acceptance test threshold determination method with controllable failure rate,” Journal of geodesy, vol. 89, no. 4, pp. 361–375, 2015.

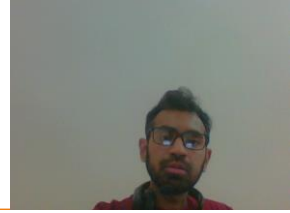

Thank you for your attention!